# A dwarf planet class object in the 21:5 resonance with Neptune

The Astrophysical Journal Letters, 855:L6 (9pp), 2018 March 1 https://doi.org/10.3847/2041-8213/aaadb3


# A Dwarf Planet Class Object in the 21:5 Resonance with Neptune

Matthew J. Holman[1], Matthew J. Payne[1], Wesley Fraser[2], Pedro Lacerda[2], Michele T. Bannister[2], Michael Lackner[3], Ying-Tung Chen (陳英同)[4], Hsing Wen Lin (林省文)[5,6], Kenneth W. Smith[2], Rosita Kokotanekova[7], David Young[2], K. Chambers[8], S. Chastel[8], L. Denneau[8], A. Fitzsimmons[2], H. Flewelling[8], Tommy Grav[9], M. Huber[8], Nick Induni[1], Rolf-Peter Kudritzki[8], Alex Krolewski[1], R. Jedicke[8], N. Kaiser[8], E. Lilly[8], E. Magnier[8], Zachary Mark[1], K. J. Meech[8], M. Micheli[8], Daniel Murray[10], Alex Parker[11], Pavlos Protopapas[3], Darin Ragozzine[12], Peter Veres[1], R. Wainscoat[8], C. Waters[8], and R. Weryk[8]

[1] Harvard-Smithsonian Center for Astrophysics, 60 Garden Street, MS 51, Cambridge, MA 02138, USA; mholman@cfa.harvard.edu
[2] Astrophysics Research Centre, School of Mathematics and Physics, Queen's University Belfast, Belfast BT7 1NN, UK
[3] Institute for Applied Computational Science, Harvard University, Cambridge, MA, USA
[4] Institute of Astronomy and Astrophysics, Academia Sinica, 11F of AS/NTU Astronomy-Mathematics Building, No. 1 Roosevelt Road, Sec. 4, Taipei 10617, Taiwan
[5] Institute of Astronomy, National Central University, Taoyuan 32001, Taiwan
[6] Department of Physics, University of Michigan, Ann Arbor, MI 48109, USA
[7] Max Planck Institute for Solar System Research, Justus-von-Liebig-Weg 3, D-37077 Göttingen, Germany
[8] Institute for Astronomy, University of Hawaii, 2680 Woodlawn Drive, Honolulu, HI 96822, USA
[9] Planetary Science Institute, Tucson, AZ 85719, USA
[10] Department of Physics, University of Wisconsin, Milwaukee, WI 53211, USA
[11] Southwest Research Institute, Department of Space Studies, Boulder, CO 80302, USA
[12] Brigham Young University, Department of Physics and Astronomy, Provo, UT 84602, USA
*Received 2017 September 12; revised 2018 January 12; accepted 2018 February 3; published 2018 February 28*

## Abstract

We report the discovery of an $H_r = 3.4 \pm 0.1$ dwarf planet candidate by the Pan-STARRS Outer Solar System Survey. 2010 $JO_{179}$ is red with $(g - r) = 0.88 \pm 0.21$, roughly round, and slowly rotating, with a period of 30.6 hr. Estimates of its albedo imply a diameter of 600–900 km. Observations sampling the span between 2005 and 2016 provide an exceptionally well determined orbit for 2010 $JO_{179}$, with a semimajor axis of 78.307 ± 0.009 au; distant orbits known to this precision are rare. We find that 2010 $JO_{179}$ librates securely within the 21:5 mean-motion resonance with Neptune on 100 Myr timescales, joining the small but growing set of known distant dwarf planets on metastable resonant orbits. These imply a substantial trans-Neptunian population that shifts between stability in high-order resonances, the detached population, and the eroding population of the scattering disk.

*Key words:* Kuiper belt objects: individual (2010 $JO_{179}$)

## 1. Introduction

Dwarf planets in the trans-Neptunian region are remnant planetesimals from the protoplanetary disk of the solar system. They constrain the large-diameter end of the trans-Neptunian object (TNO) size distribution, which is inferred from the observed luminosity function (Brown 2008; Petit et al. 2008; Schwamb et al. 2013; Fraser et al. 2014). There is no simple size cut between dwarf planet and medium-sized TNO; whether an object achieves ellipsoidal hydrostatic equilibrium is dependent on its internal ice/rock fractional composition (Tancredi & Favre 2008; Lineweaver & Norman 2010). However, few suitably sizable worlds are yet known:[13] 33 with, as a loose guide, absolute magnitude $H_V < 4$.

TNOs are faint due to their >30 au heliocentric distances, requiring discovery surveys by >1 m aperture wide-field optical telescopes. Past wide-area surveys have completed the inventory of bright TNOs to $m_r \sim 19.5$ outside the galactic plane (Tombaugh 1961; Kowal 1989; Sheppard et al. 2000; Trujillo & Brown 2003; Moody 2004; Brown 2008; Brown et al. 2015). Substantial areas of sky have been surveyed to $m_r \sim 21.5$ and deeper (Larsen et al. 2001, 2007; Elliot et al. 2005; Schwamb et al. 2010; Petit et al. 2011, 2017; Sheppard et al. 2011; Rabinowitz et al. 2012; Sheppard & Trujillo 2016; Gerdes et al. 2017).

As often the brightest and thus easiest to detect of the worlds in the trans-Neptunian region, dwarf planets also provide a useful broad-brush indication of the phase space of their dynamical populations. They are key to exploring the fainter, large-semimajor-axis populations where the smaller TNOs are too faint to detect; for example, the 2003 discovery of (90377) Sedna indicated a substantial population of TNOs with large perihelion distances (Brown et al. 2004). The $a \gtrsim 50$ au populations are all defined by their degree of gravitational interaction with Neptune: they include orbits librating in high-order mean-motion resonance (MMR); the scattering disk, on orbits actively interacting with Neptune; and the "detached" TNOs, with perihelia $q \gtrsim 37$ au (Gladman et al. 2008). Recent discoveries include the 9:2 mean-motion resonant object 2015 $RR_{245}$ with $H_r = 3.6$ and $a = 81.86 \pm 0.05$ au (Bannister et al. 2016a), the scattering disk TNO 2013 $FY_{27}$ with $H_V = 2.9$ and $a = 59$ au (Sheppard & Trujillo 2016), and the detached TNO 2014 $UZ_{224}$ with $H_V = 3.5$ and $a = 109 \pm 7$ au (Gerdes et al. 2017).

The Panoramic Survey Telescope and Rapid Response System 1 Survey (Pan-STARRS 1, hereafter PS1) is well suited to the discovery of TNOs. PS1 is a 1.8 m telescope on Haleakela in Hawai'i, with a dedicated 0.″258 pixel, 7 $deg^2$ optical imager

[13] http://www.minorplanetcenter.net/db_search: $a \geqslant 30$, $q \geqslant 30$, and $H_V \leqslant 4$, as of 2018 February 21.

(Kaiser et al. 2010; Chambers et al. 2016). The PS1 3$\pi$ survey (Magnier et al. 2013; Chambers et al. 2016) repeatedly observed the sky north of decl. $-30°$ using a Sloan-like filter system (Tonry et al. 2012), reaching typical single-exposure $5\sigma$ depths of $g_{P1} = 22.0$, $r_{P1} = 21.8$, and $i_{P1} = 21.5$ (see Table 11 of Chambers et al. 2016). PS1 also observed within $\pm 20°$ of the ecliptic using the wide $w_{P1}$ filter ($m_{5\sigma} \sim 22.5$). The observing cadence of PS1 is optimized for detection of inner solar system minor planets, with analysis for detection made with the PS Moving Object Processing System (MOPS; Denneau et al. 2013). However, PS1's many visits permit detection of slower-moving ($\sim 3''$/hr) TNOs in the accumulated data. Weryk et al. (2016) reported several hundred centaurs and TNOs from a search of the 2010 February 24 to 2015 July 31 PS1 observations, which linked together detections within 60 day intervals.

The PS1 outer solar system (OSS) key project uses a novel linking solution, based on transforming topocentric observations to a heliocentric coordinate frame using an *assumed* heliocentric distance. Our initial search of the 2010–2014 PS1 observations resulted in hundreds of candidates, ~50% of which were newly discovered TNOs (Holman et al. 2015). These include unusual objects such as the highly inclined centaur (471325) 2011 $KT_{19}$ (Chen et al. 2016), as well as numerous new Neptune trojans (Lin et al. 2016).

Here, we report the discovery of an $m_r \sim 21$ dwarf planet candidate at a barycentric distance of 55 au: 2010 $JO_{179}$. We present the technique used to detect 2010 $JO_{179}$ (Section 2), our observations (Section 3), 2010 $JO_{179}$'s physical properties (Section 4), the dynamical classification of its orbit (Section 5), and the broader implications of its existence for our understanding of the distant, dynamically excited TNO populations (Section 6).

## 2. TNO Discovery Technique

We developed our discovery pipeline to cope with the temporal sparsity of the Pan-STARRS data (see Brown et al. 2015 for an independent, alternative approach to detecting TNOs in sparse data sets). Our pipeline operates on the catalogs of source detections found in the direct, undifferenced PS1 exposures spanning 2010 to mid-2014 by the Image Processing Pipeline (IPP; Magnier 2006, 2007). We eliminate any detection that coincides within $1''$ of a known stationary source. (A catalog of stationary sources was developed from the individual detections in the PS1 exposures; detections that occur near the same location over multiple nights are considered to be stationary.) The remaining transient detections form the input to the rest of the pipeline (we do not use MOPS). All magnitudes are transformed to *w*-band (Tonry et al. 2012) for uniformity of comparison. We iterate over a set of heliocentric distances, $d \sim 25$–$1500$ au. For each assumed distance, we carry out a number of steps. First, we transform the topocentric sky plane positions of transient sources we identify in the PS1 imaging to those as would be observed from the Sun. Then, all *tracklets* are identified: these are sets of $\geqslant 2$ detections from the exposures within each individual night that are consistent with linear motion that would be bound to the Sun. No minimum rate of motion is required. Tracklets with three or more detections are much more likely to be real, as the positions of their constituent detections must be consistent with linear motion at a constant rate. For every pair of high-confidence tracklets ($\geqslant 3$ detections) that can be associated with a bound heliocentric orbit, we look for additional supporting tracklets along the great circle defined by those two tracklets. If an additional tracklet is found, an orbit is fit (using modified routines from the Orbfit package of Bernstein & Khushalani 2000) to the set of observations from those three tracklets, and a search is carried out for additional tracklets along the sky plane trajectory defined by that orbit. As tracklets are found, the orbit is refined and the search continues, recursively. All of the different linking possibilities are followed until the set of plausibly connected tracklets is exhausted. As a final step, single detections that lie within $1\farcs0$ of the sky plane are searched for and incorporated, with astrometric and photometric outliers rejected.

We consider for further investigation any arc of tracklets with detections on at least five separate nights that has an orbital solution with a reduced chi-squared $\bar{\chi}^2 \lesssim 3$ and that has a range of observation magnitudes that is physically realistic ($\Delta m_w < 1.5$). All directions of motion of the resulting orbit are permitted and retained.

## 3. Observations

The observations of 2010 $JO_{179}$ span 12 oppositions. All available photometry is tabulated in the Appendix (Table 3); the astrometry is listed at the Minor Planet Center.[14]

We initially detected 2010 $JO_{179}$ in *g*-, *r*-, and *i*-band observations spanning 2010–2012 from the PS1 3$\pi$ survey (Table 3). The absence of *w*-band observations is due to 2010 $JO_{179}$'s 32° ecliptic latitude at the time of discovery, outside the coverage of the PS1 *w*-band survey. 2010 $JO_{179}$ is seen on 12 distinct nights with a total of 24 detections, forming an arc spanning 790 days. 2010 $JO_{179}$ was retained as a candidate TNO as it passed two tests: (a) the residuals to an orbital solution determined with a modified version code of Bernstein & Khushalani (2000) were consistent with the astrometric uncertainties of the individual detections ($\sim 0\farcs1$), with no outliers; (b) the photometric measurements from the PS1 IPP, transformed to *w*-band (Tonry et al. 2012), spanned only 1.2 mag. We visually examined the detections in the PS1 images for final verification that each was genuine. The photometry in Table 3 is calibrated PS1 Data Release 1 (PS1-DR1; Magnier et al. 2016) and was measured with the moving-object photometry analysis package TRIPPy (Fraser et al. 2016).

Although 2010 $JO_{179}$ is substantially brighter than the PS1 detection limits, there is a significant bias against finding such objects with the algorithm we described in Section 2. First, we note that only two tracklets with three or more detections can be seen in Table 3. This is the minimum number for our algorithm. If either of these tracklets was removed from the data set, the algorithm would not have found 2010 $JO_{179}$. This could occur moderately often, given the 76% fill factor of the focal plane (Chambers et al. 2016). Interestingly, the later of those two tracklets was *accidental*: it was found in the overlap between two adjacent fields for which pairs of observations were being taken. The overlap region is 10%–20% of the survey area, depending upon the specific survey pattern.

We followed up 2010 $JO_{179}$ with Sloan *r*-band observations on 2016 July 28–30 with the EFOSC2 camera on the New Technology Telescope (NTT; Buzzoni et al. 1984; Snodgrass et al. 2008) atop La Silla, Chile. EFOSC2 uses a LORAL $2048 \times 2048$ CCD that was used in $2 \times 2$ binning mode. Each binned pixel maps onto an on-sky square $0\farcs24$ on the side, for a full field of view $4\farcm1 \times 4\farcm1$. The data were subject to standard bias-subtraction and flat-fielding procedures, and the magnitude of

[14] M.P.E.C. 2017-S54: http://www.minorplanetcenter.net/mpec/K17/K17S54.html

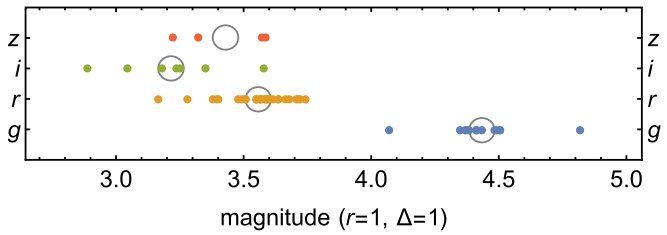


**Figure 1.** 2010 $JO_{179}$ magnitudes in each band corrected to unit heliocentric and geocentric distance. Gray circles indicate mean magnitudes.

2010 $JO_{179}$ in each frame was measured using circular aperture photometry and calibrated to PS1-DR1 using tens of field stars.

2010 $JO_{179}$ is bright enough to be found in archival images with the SSOIS search tool (Gwyn et al. 2012). We recovered astrometry of 2010 $JO_{179}$ from the *griz* observations of a sequence of 54 s exposures (*riuzg*) made on 2005 May 11. The observations by the 2.5 m telescope of the Sloan Digital Sky Survey (SDSS) in New Mexico were part of SDSS-II (Abazajian et al. 2009). The astrometry of the 0.″396 pixel images is calibrated to SDSS Data Release 14 (Abolfathi et al. 2017). The TNO was close by stars, which prevented photometric measurements.

We also found via SSOIS that 2010 $JO_{179}$ was serendipitously imaged in Sloan $g$, $r$, and $z$ on 2014 August 16–18 by the DECalS survey[15] with the Dark Energy Camera (DECam; DePoy et al. 2008) on the 4 m Blanco Telescope in Chile. DECam has 0.″263 pixels with a 3 $deg^2$ field of view. The DECalS astrometry and photometry zeropoints are calibrated[16] to PS1-DR1. The five highest signal-to-noise ratio (S/N) and best seeing DECam images are our overall highest-S/N images of 2010 JO179. Photometry, point-spread function (PSF) modeling, and trailed PSF removal were performed with TRIPPy (Table 3). No evidence of binarity was found, to an estimated signal-to-noise ratio (S/N) = 5 detection threshold and a separation of ∼1 FWHM.

## 4. Physical Properties of 2010 $JO_{179}$

The mean colors of 2010 $JO_{179}$ were calculated from the mean magnitudes in each band, after correction to unit heliocentric and geocentric distance (Figure 1). Standard deviations for each band were combined in quadrature to yield the uncertainty. Table 1 summarizes the derived color measurements. The substantial time between observations means rotation could have let potential surface variability intrude (Fraser et al. 2015; Peixinho et al. 2015), so we avoid presenting the colors as a coarsely sampled spectrum. The $g - r$ and $r - i$ of 2010 $JO_{179}$ fall along the locus of the known range of TNOs (e.g., Ofek 2012), classing it as moderately red.[17]

The visual albedos constrained by thermal measurements for $2 < H_r < 4$ TNOs are wide-ranging, varying from $p = 0.07$–$0.21$ (Brucker et al. 2009; Lellouch et al. 2013; Fraser et al. 2014). As the color-albedo clustering seen for smaller TNOs does not continue to objects this large (Lacerda et al. 2014; Fraser et al. 2014), the albedo of 2010 JO179 is unconstrained within the known albedo range. At

[15] http://legacysurvey.org/decamls/
[16] http://legacysurvey.org/dr3/description/
[17] Relative to solar color $g - r = 0.44 \pm 0.02$: sdss.org/dr12/algorithms/ugrizvegasun/.

**Table 1**
Optical Colors of 2010 $JO_{179}$

| Facility | MJD | $g - r$ | $r - i$ | $r - z$ |
|---|---|---|---|---|
| Mean | | | | |
| All | | 0.88 ± 0.21 | 0.34 ± 0.26 | 0.13 ± 0.22 |
| Single-epoch | | | | |
| PS1 | 55711.36 | 1.2 ± 0.12 | | |
| DECam | 56886.00 | | | −0.09 ± 0.25 |
| NTT | 57597.13 | 0.95 ± 0.13 | | |
| NTT | 57599.01 | 0.85 ± 0.04 | | |
| NTT | 57599.04 | 0.74 ± 0.04 | | |
| NTT | 57599.08 | 0.78 ± 0.03 | | |

**Note.** For computation of mean color, see Section 4.

$H_r = 3.44 \pm 0.10$ (see below), 2010 $JO_{179}$ has a diameter of at least 600 km; at the less reflective albedo limit, it could be as large as 900 km. It will thus achieve ellipsoidal hydrostatic equilibrium (Tancredi & Favre 2008; Lineweaver & Norman 2010).

2010 $JO_{179}$'s $r - z$ color is unusually blue. To make it consistent with the range of $r - z$ colors exhibited by other TNOs with $g - r$ colors similar to 2010 $JO_{179}$ (Pike et al. 2017a) requires a $1\sigma$ deviation in both $g - r$ and $r - z$, or a $2\sigma$ deviation in either. Yet the mean $r - z$ is consistent with the only single-epoch $r - z$ measurement (from DECam; see Table 1). Alternatively, the negative $r - z$ color is broadly consistent with the presence of methane ice, which exhibits an absorption feature through the $z$ band (see, for example, Tegler et al. 2007). For 2010 $JO_{179}$ to have a methane-bearing surface would be unusual, as it is expected that objects of this size would rapidly lose that volatile to space on short timescales (Schaller & Brown 2007b), in contrast to the larger dwarf planets, e.g., (50000) Quaoar and 2007 $OR_{10}$ are red methane-covered objects (Schaller & Brown 2007a; Brown et al. 2011).

We use the photometry in Table 3 to constrain the color, phase curve, and light curve properties for 2010 $JO_{179}$. The apparent magnitudes were first corrected to units of heliocentric ($r$) and geocentric ($\Delta$) distance by subtraction of $5\log(r\Delta)$. The corrected $g$ and $r$ magnitudes were fit simultaneously with the following model, which accounts for a linear phase darkening and sinusoidal light curve variation:

$$H_{g,r} - (g - r) + \beta\alpha + \frac{\Delta m}{2}\sin\left[\frac{2\pi(t - t_0)}{P}\right], \qquad (1)$$

where $H_{g,r}$ is the absolute $g$ or $r$ magnitude; $\alpha$ is the phase angle; $\beta$ is the linear phase function slope; $\Delta m$, $P$, and $t_0$ are the peak-to-peak variation, period, and offset of the light curve, respectively; and $(g - r)$ is a color term subtracted from the $g$ magnitudes only. As is the case for Earth-based TNO observations, the range of phase angle is limited: $0 < \alpha \lesssim 1°$. We found the best-fit $\beta$ to be somewhat dependent on the initialization values for $P$, $\Delta m$, and $\beta$. To solve this, we varied $(g - r)$ linearly in steps of 0.01 mag and at each step generated 200 uniformly distributed random initial values $P \in (16, 64)$, $\Delta m \in (0.15, 0.60)$, and $\beta \in (0.01, 0.50)$. The range of $\beta$ values brackets the slopes seen in TNOs (Rabinowitz et al. 2007).

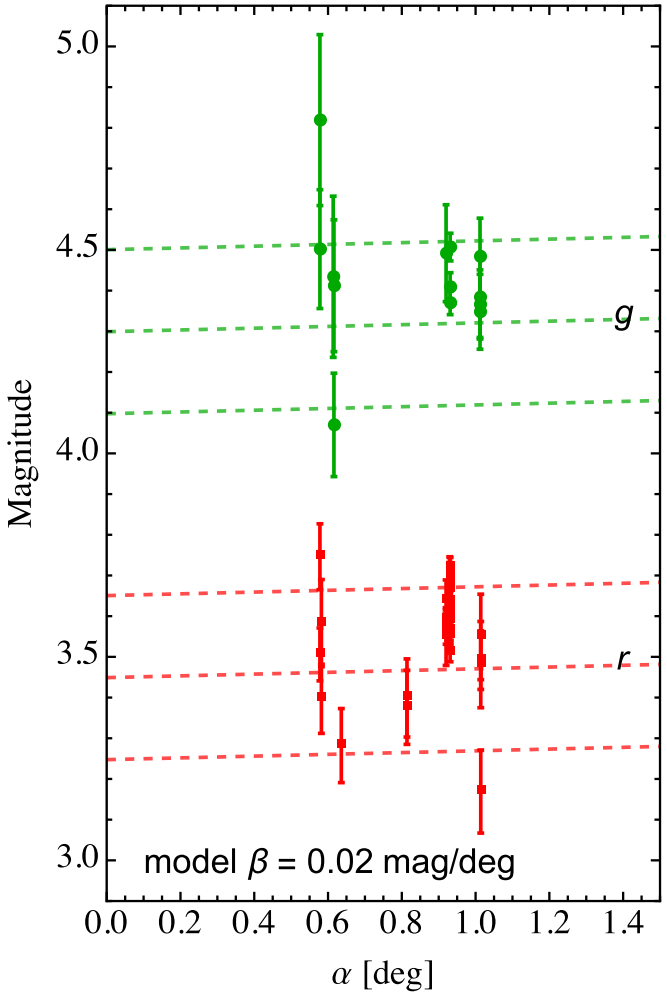


**Figure 2.** Linear phase curve models for 2010 $JO_{179}$. The slope $\beta = 0.02$ mag deg$^{-1}$ ($\beta < 0.07$ mag deg$^{-1}$, $1\sigma$) was fit simultaneously to the $g$ and $r$ photometry (Table 3). The dashed lines mark the mean brightness and extent of the variation due to the light curve (see Figure 3).

The NTT $r$-band photometry displays a steady brightening by about 0.2 mag over a period of 5 hr, which provides useful limits on the light curve variation ($\Delta m > 0.2$ mag) and period ($P > 10$ hr). We found consistently that shallow phase functions ($\beta < 0.05$ mag deg$^{-1}$) fit the data best (see Figure 2). For this reason we decided not to correct the data for phase effects before the light curve analysis.

We employed the Lomb–Scargle algorithm (Press & Rybicki 1989) to measure the light curve period using the $r$-band measurements only. The periodogram identified the period $P_1 = 30.6324$ hr as the best solution, which corresponds to a single-peaked light curve, with one maximum and one minimum per rotation. Figure 3 shows the data phased with $P_1$. The double period $P_2 = 2P_1 = 61.2649$ hr is also shown for comparison, in case 2010 $JO_{179}$ has a symmetric light curve.

Both the solutions are consistent with the data and indicate that 2010 $JO_{179}$ is a slow rotator. The single-peaked solution, $P \sim 30.6$ hr, would imply that 2010 $JO_{179}$ is roughly spherical and has significant albedo patchiness. The double-peaked solution would imply an ellipsoidal shape with axes ratio $a/b > 1.58$. We find this less plausible, given the large size and slow rotation of 2010 $JO_{179}$.

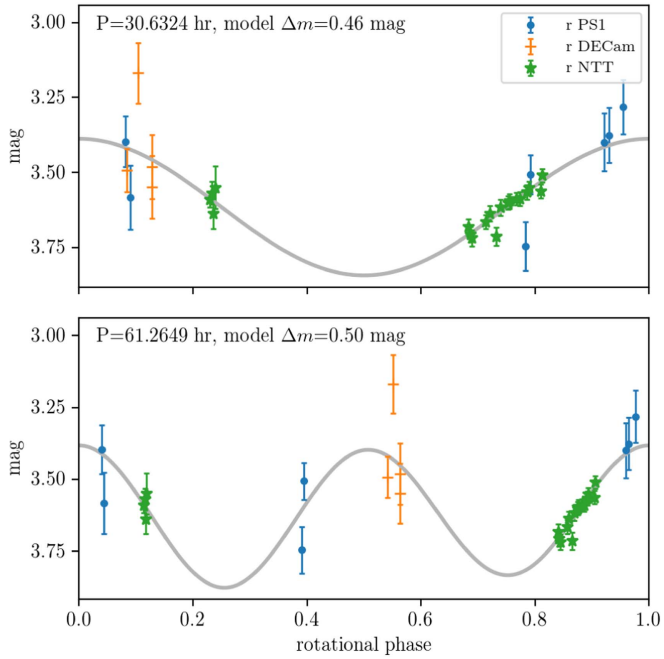


**Figure 3.** Light curve of $r$-band photometry of 2010 $JO_{179}$, color-coded by observing facility (Table 3). The single-peaked model implies a nearly spherical shape with a patchy surface spinning with a period $P \approx 32.5$ hr. The corresponding double-peaked solution (period $P \approx 65$ hr) implying an ellipsoidal shape with axes ratio $a/b > 1.58$ is less plausible, due to the large material strength required to hold the shape against the crush of gravity.

Finally, the light curve period solutions were used to refine the phase curve, resulting in the linear solution shown in Figure 2, with $\beta = 0.02$ mag deg$^{-1}$. We force $\beta > 0$ in our fitting algorithm, which sets the lower limit on the phase function slope, and find a $1\sigma$ upper limit $\beta < 0.07$ deg mag$^{-1}$. We find an absolute $r$ magnitude $H_r = 3.44 \pm 0.10$ and a best-fit color offset $g - r = 0.85$, consistent with the $g - r$ values in Table 1.

## 5. Orbital Dynamics of 2010 $JO_{179}$

We determine the barycentric elements of 2010 $JO_{179}$ by fitting observations from six oppositions spanning 2005–2016 (Table 2), using the code of Bernstein & Khushalani (2000). The barycentric distance to 2010 $JO_{179}$ at discovery in 2010 is $55.019 \pm 0.003$ au.

We generate 100 clones of the orbit of 2010 $JO_{179}$, varying the observations by their respective uncertainties and refitting the orbit, hence creating a statistically rigorous bundle of orbits that are all consistent with the observations. We integrate the best-fit orbit and clones as test particles in a barycentric system, orbiting in the gravitational field of the Sun and four giant planets. We integrate the particles using the adaptive IAS15 integrator (Rein & Spiegel 2015) in the REBOUND code of Rein & Liu (2012) for 700 Myr, i.e., around $10^6$ orbits of 2010 $JO_{179}$.

The period ratios with Neptune, eccentricity and inclination for the best-fit orbit (black), and a sample of the clones (all other colors) are shown in the top three panels of Figure 4. All of the particles stably orbit with period ratios very close to 4.2.

**Table 2**
Barycentric Osculating Elements of 2010 $JO_{179}$ in the International Celestial Reference System at Epoch 2455327.1

| $a$ (au) | $e$ | $i$ (°) | $\Omega$ (°) | $\omega$ (°) | $T_{\rm peri}$ (JD) |
|---|---|---|---|---|---|
| 78.307 ± 0.009 | 0.49781 ± 0.00005 | 32.04342 ± 0.00001 | 147.1722 ± 0.0002 | 9.824 ± 0.005 | 2433937.1 ± 0.8 |

**Note.** Best-fit orbit to the arc of observations 2005–2016 with the method of Bernstein & Khushalani (2000), with $1\sigma$ uncertainty estimates from the covariance matrix.

We then consider the resonant angle,

$$\theta_{p+q:q} = (p+q)\lambda_{\rm out} - p\lambda_{\rm in} - q\varpi_{\rm out}, \quad (2)$$

and plot in the lower panel of Figure 4 values for Equation (2) using $p+q{:}p = 21{:}5$. The best-fit orbit exhibits stable libration in the 21:5 resonance for ∼100 Myr before diffusing to a circulating configuration with a period ratio ∼4.21 with respect to Neptune for ∼300 Myr, before returning to a 21:5 resonant configuration for the remainder of the simulation. We note that 16 possible resonant angles exist for the 21:5 resonance in which the $-q\varpi_{\rm out}$ term in Equation (2) is replaced by $-(n\varpi_{\rm in} + (q-n)\varpi_{\rm out})$, with $0 \leqslant n \leqslant 15$. We examined all such variations for all best-fit and clone orbits, and found that only the $n = 0$ case (i.e., Equation (2)) ever exhibits resonance.

The clones of the orbit of 2010 $JO_{179}$ display behavior consistent with that of the best-fit orbit. For the entirety of the simulation, all clones have period ratios with Neptune that remain bounded between 4.185 and 4.215 (semimajor axes bounded between ∼78.1 au and ∼78.5 au) and have pericenters in the range 37.5–41.5 au. The narrowness of the 21:5 resonance means even the small remaining orbital uncertainties encompassed by the clones are of similar scale to structures in the resonance's phase space. Most clones move back and forth between resonant and non-resonant configurations, with a slow overall diffusion away from resonance. *All* clones are resonant at the start of the simulation, and ∼6% remain resonant for the entire simulation, so there is some possibility that 2010 $JO_{179}$ is on one of these stable orbits. The median time at which clones exit resonance is ∼110 Myr. At 700 Myr, ∼25% of clones are resonant.

From the majority behavior of the best-fit orbit and its clones over the 700 Myr simulation, 2010 $JO_{179}$ probably has a metastable orbit, which switches between resonant and non-resonant configurations on hundred-Myr timescales.

## 6. Discussion

Although 2010 $JO_{179}$ is bright for a TNO at $m_r \sim 21$, its 32° orbital inclination (Figure 5, right) and resulting current ∼30° ecliptic latitude is responsible for it not being detected earlier. It is bright enough to have been detected by the surveys of Larsen et al. (2007) and Schwamb et al. (2010), but fell just outside their sky coverage. It was not detected by Weryk et al. (2016), presumably either because 2010 $JO_{179}$ is outside of the region considered in that search, or it was not observed with their required cadence. 2010 $JO_{179}$ is thus a good example of how the detection efficiency of a survey is a function of each specific analysis, given a common observational data set. Surveys that cover large fractions of the sky, both well away from the ecliptic and to fainter limiting magnitudes, such as are planned for the forthcoming Large Synoptic Survey Telescope (LSST; Science Collaboration et al. 2009), will discover many more such objects. However, archival data will clearly still yield new discoveries with further thorough searching.

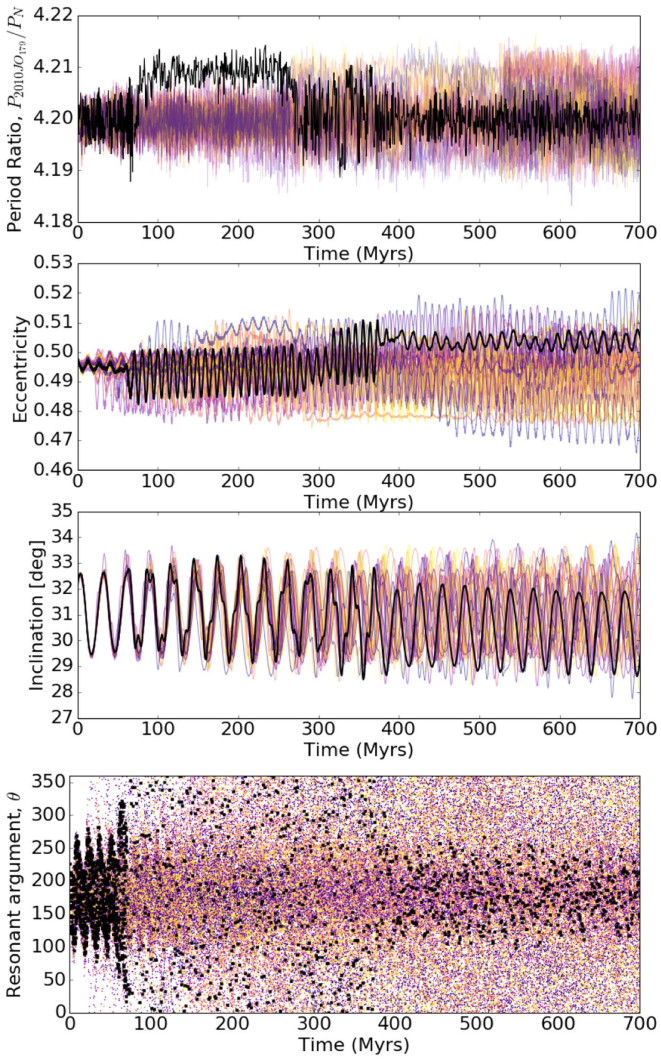


**Figure 4.** Dynamical evolution of the best-fit orbit for 2010 $JO_{179}$ (black) and clones (colors) sampled from the covariance matrix of the orbital uncertainties. Top panel: period ratio with Neptune; second panel: eccentricity; third panel: inclination; bottom panel: resonance angle, $\theta$ (see Equation (2)). The best-fit orbit stably librates in the 21:5 resonance with Neptune for ∼70 Myr, before diffusing to a circulating state, and then back to librating. The clones exhibit behavior consistent with that of the best-fit orbit, switching between resonant and non-resonant configurations on ∼100 Myr timescales, with a slow diffusion away from resonance, such that at 700 Myr, ∼25% remain in resonance.

For population studies, the detection efficiency of surveys such as PS1 need to be well characterized, as has been done for the CFEPS and OSSOS surveys (Petit et al. 2011; Bannister et al. 2016b), to be able to correct for the observational biases. In addition, detailed dynamical classifications of the discoveries, of the type we have done here, need to be made. These permit determination of the intrinsic abundance of TNOs such as

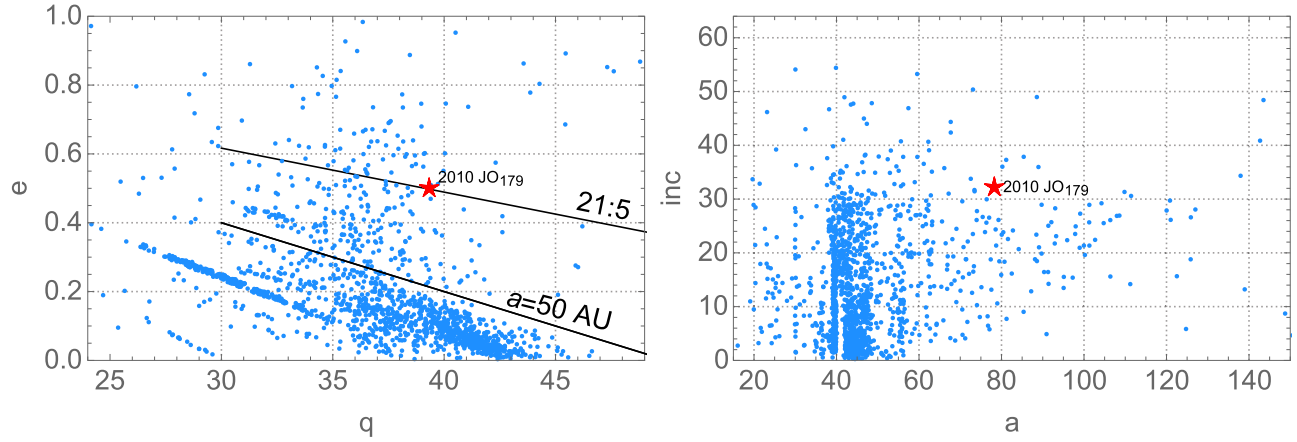


**Figure 5.** 2010 $JO_{179}$ (red star) placed in context among the other known TNOs (blue dots; those listed in the MPC with multiple oppositions of observations, on orbits with $q > 15$ au).

2010 $JO_{179}$ (e.g., Pike et al. 2015). This is the subject of future work with PS1.

With a perihelion distance $q = 39.32$ au (Figure 5), near the boundary between what are considered to be low perihelion and high perihelion TNOs (Lykawka & Mukai 2007a; Gladman et al. 2008), 2010 $JO_{179}$ is a relatively nearby example of what is now being recognized as a very substantial population of high-perihelion TNOs (Gladman et al. 2002; Gomes 2003; Trujillo & Sheppard 2014; Pike et al. 2015; Kaib & Sheppard 2016; Nesvorný & Vokrouhlický 2016; Nesvorný et al. 2016). In the absence of a survey characterization, we cannot provide an absolute estimate for the 21:5 resonant population, especially given the strong observability bias on the eccentricity distribution of such a large-$a$ population. However, we can find a general lower limit. The existence of 2010 $JO_{179}$ requires there to be at least one $H_r \simeq 3.5$ TNO. Scaling according to the size distribution of the dynamically excited TNOs (Fraser et al. 2014), there are at least 6700 objects in the 21:5 that are larger than 100 km in diameter. This would be more numerous than the 3:2 plutinos (Gladman et al. 2012); note the sizable known sample of this population visible in Figure 5, and is consistent with the large populations found in other distant resonances (Pike et al. 2015; Volk et al. 2016). We note that the 21:5 is not an intrinsically "special" resonance: this argument applies more generally for any large-$e$ orbit with $q \sim 39$ au (e.g. Bannister et al. 2016a), and the 21:5 occupancy only reinforces the vast scale of the populations in this region. Aspects of these large populations remain challenging to form in migration scenarios (cf. Pike et al. 2017b).

Neptune's early migration into the outer planetesimal disk plausibly emplaced the dynamically excited trans-Neptunian populations, including the resonant and scattering disk (Malhotra 1995; Gomes 2003; Gladman et al. 2008). Predicting the details of the emplaced distant populations is an area of active investigation. Nesvorný et al. (2016) and Kaib & Sheppard (2016) independently predict that some TNOs with $a > 50$ au and $q > 40$ au should exhibit semimajor axes clustered near and inward, but not within, MMRs with Neptune. This followed from modeling Neptune's dynamical evolution on an orbit with moderate $e \lesssim 0.1$ eccentricity, both under smooth migration and from "grainy" gravitational interaction with a small sea of dwarf planets in the initial planetesimal disk (Nesvorný & Vokrouhlický 2016). In direct contrast, Pike & Lawler (2017) predict fairly symmetric trails of high-perihelia populations immediately surrounding distant MMRs. They assessed emplacement by the Nice model scenario of Brasser & Morbidelli (2013), with a smoothly migrating, initially high $e = 0.3$ Neptune. While one might hope to constrain the details of migration from the present-day orbit of a distant TNO like 2010 $JO_{179}$, it unfortunately lies in a region of phase space where its orbit does not distinguish among current model outcomes. Irrespective of whether Neptune's migration was smooth or grainy, fast or slow, the results of Nesvorný et al. (2016), Kaib & Sheppard (2016), and Pike & Lawler (2017) all contain TNOs with $a \sim 78$ au, $q \sim 39$ au, $i \sim 30°$.

It is also worth considering if 2010 $JO_{179}$ could be a more recent arrival to its current orbit. The $a > 50$ au region is filigreed with high-order resonances. These permit "resonance sticking," where a TNO's orbit temporarily librates in resonance for tens to hundreds of millions of years, chaotically escapes the resonance, changing in semimajor axis, then sticks, librating within another resonance (e.g., Lykawka & Mukai 2007b). The resonant dynamics during a temporary capture can lead to oscillations in eccentricity and inclination that can then weaken the TNO's interaction with Neptune (Gomes et al. 2008; Sheppard et al. 2016). However, 2010 $JO_{179}$'s clones all remain close to its resonance (Section 5), implying stability for the age of the solar system, rather than showing behavior like that of 2015 $RR_{245}$, which moves between the 9:2 resonance and the scattering disk (Bannister et al. 2016a). 2010 $JO_{179}$'s clones exhibit similar behavior to the four known TNOs in and by the 5:1 resonance at $a \sim 88$ au (Pike et al. 2015). The current orbit of 2010 $JO_{179}$ is therefore more likely to be ancient.

M.J.H. and M.J.P. gratefully acknowledge NASA Origins of Solar Systems Program grant NNX13A124G and grant NNX10AH40G via sub-award agreement 1312645088477, BSF Grant 2012384, NASA Solar System Observations grant NNX16AD69G, as well as support from the Smithsonian 2015 CGPS/Pell Grant program. M.T.B. appreciates support from UK STFC grant ST/L000709/1.

The Pan-STARRS 1 Surveys (PS1) have been made possible through contributions of the Institute for Astronomy, the University of Hawaii, the Pan-STARRS Project Office, the Max-Planck Society and its participating institutes, the Max

Planck Institute for Astronomy, Heidelberg and the Max Planck Institute for Extraterrestrial Physics, Garching, The Johns Hopkins University, Durham University, the University of Edinburgh, Queen's University Belfast, the Harvard-Smithsonian Center for Astrophysics, the Las Cumbres Observatory Global Telescope Network Incorporated, the National Central University of Taiwan, the Space Telescope Science Institute, the National Aeronautics and Space Administration under grant No. NNX08AR22G issued through the Planetary Science Division of the NASA Science Mission Directorate, the National Science Foundation under grant No. AST-1238877, the University of Maryland, and Eotvos Lorand University (ELTE).

This work is based in part on observations collected at the European Organisation for Astronomical Research in the Southern Hemisphere under ESO programmes 194.C-0207 (H), and on observations at Cerro Tololo Inter-American Observatory, National Optical Astronomy Observatory, which is operated by the Association of Universities for Research in Astronomy (AURA) under a cooperative agreement with the National Science Foundation.

The computations in this Letter were run on the Odyssey cluster supported by the FAS Science Division Research Computing Group at Harvard University.

This research used the facilities of the Canadian Astronomy Data Centre operated by the National Research Council of Canada with the support of the Canadian Space Agency.

*Facilities:* PS1, NTT (EFOSC2), Sloan, CTIO:Blanco (DECam).

*Software:* Astropy, TRIPPy, REBOUND, Matplotlib.

## Appendix
## Observational Data

The Appendix comprises Table 3.

**Table 3**
Photometry of 2010 $JO_{179}$

| Date (UTC) | Date (MJD) | Filter | $m_{\rm filter}$ | Exp (s) | Facility |
|---|---|---|---|---|---|
| 2010 May 10 13:51:55.9 | 55326.577730 | i | 20.62 ± 0.10 | 45 | PS1 |
| 2010 May 10 14:08:27.7 | 55326.589210 | i | 20.26 ± 0.10 | 45 | PS1 |
| 2010 May 11 13:50:39.0 | 55327.576840 | r | 20.77 ± 0.09 | 40 | PS1 |
| 2010 May 11 14:07:02.2 | 55327.588220 | r | 20.95 ± 0.11 | 40 | PS1 |
| 2010 Jun 04 08:19:36.5 | 55351.346950 | i | 20.95 ± 0.09 | 45 | PS1 |
| 2010 Jun 04 08:21:36.6 | 55351.348340 | i | 20.61 ± 0.07 | 45 | PS1 |
| 2010 Jun 04 08:37:05.4 | 55351.359090 | i | 20.73 ± 0.08 | 45 | PS1 |
| 2010 Jun 04 08:39:04.6 | 55351.360470 | i | 20.55 ± 0.07 | 45 | PS1 |
| 2010 Jun 08 11:51:56.2 | 55355.494400 | r | 20.66 ± 0.09 | 40 | PS1 |
| 2010 Jul 01 10:15:11.8 | 55378.427220 | r | 20.78 ± 0.10 | 40 | PS1 |
| 2010 Jul 01 10:31:53.2 | 55378.438810 | r | 20.76 ± 0.09 | 40 | PS1 |
| 2011 May 30 08:33:38.9 | 55711.356700 | g | 22.22 ± 0.21 | 43 | PS1 |
| 2011 May 30 08:48:54.7 | 55711.367300 | g | 21.91 ± 0.15 | 43 | PS1 |
| 2011 May 30 09:05:46.5 | 55711.379010 | r | 21.15 ± 0.08 | 40 | PS1 |
| 2011 May 30 09:20:08.7 | 55711.388990 | r | 20.91 ± 0.07 | 40 | PS1 |
| 2011 Jun 07 12:20:36.4 | 55719.514310 | g | 21.48 ± 0.13 | 43 | PS1 |
| 2011 Jun 07 12:35:18.5 | 55719.524520 | g | 21.82 ± 0.16 | 43 | PS1 |
| 2011 Aug 15 08:10:48.6 | 55788.340840 | i | 20.48 ± 0.21 | 45 | PS1 |
| 2012 Jun 08 08:00:09.2 | 56086.333440 | g | 21.87 ± 0.20 | 43 | PS1 |
| 2014 Aug 16 00:22:58.0 | 56885.015949 | g | 22.02 ± 0.09 | 84 | DECam |
| 2014 Aug 16 01:07:29.5 | 56885.046869 | g | 21.90 ± 0.09 | 88 | DECam |
| 2014 Aug 16 01:37:17.4 | 56885.067563 | g | 21.92 ± 0.10 | 82 | DECam |
| 2014 Aug 16 01:48:27.6 | 56885.075320 | g | 21.88 ± 0.09 | 87 | DECam |
| 2014 Aug 16 23:11:35.6 | 56885.966385 | z | 21.12 ± 0.24 | 122 | DECam |
| 2014 Aug 17 00:09:24.4 | 56886.006532 | r | 21.03 ± 0.07 | 70 | DECam |
| 2014 Aug 17 00:43:23.8 | 56886.030136 | r | 20.70 ± 0.10 | 72 | DECam |
| 2014 Aug 17 01:28:22.7 | 56886.061374 | r | 21.02 ± 0.11 | 69 | DECam |
| 2014 Aug 17 01:30:00.8 | 56886.062509 | r | 21.08 ± 0.10 | 71 | DECam |
| 2014 Aug 18 00:29:15.7 | 56887.020321 | z | 20.86 ± 0.09 | 121 | DECam |
| 2014 Aug 18 01:29:05.1 | 56887.061864 | z | 20.76 ± 0.10 | 124 | DECam |
| 2014 Aug 18 01:31:38.7 | 56887.063642 | z | 21.11 ± 0.13 | 127 | DECam |
| 2016 Jul 28 02:51:47.5 | 57597.119300 | r | 21.18 ± 0.03 | 300 | NTT |
| 2016 Jul 28 02:57:24.5 | 57597.123200 | r | 21.15 ± 0.04 | 300 | NTT |
| 2016 Jul 28 03:03:01.4 | 57597.127100 | r | 21.22 ± 0.05 | 300 | NTT |
| 2016 Jul 28 03:08:55.7 | 57597.131200 | r | 21.13 ± 0.07 | 300 | NTT |
| 2016 Jul 28 03:14:32.6 | 57597.135100 | g | 22.08 ± 0.12 | 300 | NTT |
| 2016 Jul 29 23:24:08.6 | 57598.975100 | r | 21.27 ± 0.03 | 300 | NTT |
| 2016 Jul 29 23:29:37.0 | 57598.978900 | r | 21.29 ± 0.03 | 300 | NTT |
| 2016 Jul 29 23:35:13.9 | 57598.982800 | r | 21.30 ± 0.03 | 300 | NTT |
| 2016 Jul 30 00:20:26.9 | 57599.014200 | r | 21.25 ± 0.02 | 300 | NTT |
| 2016 Jul 30 00:26:12.5 | 57599.018200 | g | 22.09 ± 0.03 | 300 | NTT |
| 2016 Jul 30 00:31:58.1 | 57599.022200 | r | 21.22 ± 0.03 | 300 | NTT |
| 2016 Jul 30 00:54:08.6 | 57599.037600 | r | 21.30 ± 0.03 | 300 | NTT |
| 2016 Jul 30 00:59:54.2 | 57599.041600 | g | 21.99 ± 0.04 | 300 | NTT |

**Table 3**
(Continued)

| Date (UTC) | Date (MJD) | Filter | $m_{\rm filter}$ | Exp (s) | Facility |
|---|---|---|---|---|---|
| 2016 Jul 30 01:05:31.2 | 57599.045500 | r | 21.20 ± 0.03 | 300 | NTT |
| 2016 Jul 30 01:31:35.0 | 57599.063600 | r | 21.19 ± 0.02 | 300 | NTT |
| 2016 Jul 30 01:36:11.5 | 57599.066800 | r | 21.18 ± 0.03 | 300 | NTT |
| 2016 Jul 30 01:58:39.4 | 57599.082400 | r | 21.17 ± 0.02 | 300 | NTT |
| 2016 Jul 30 02:04:25.0 | 57599.086400 | g | 21.95 ± 0.03 | 300 | NTT |
| 2016 Jul 30 02:10:10.6 | 57599.090400 | r | 21.17 ± 0.02 | 300 | NTT |
| 2016 Jul 30 02:33:04.3 | 57599.106300 | r | 21.15 ± 0.03 | 300 | NTT |
| 2016 Jul 30 02:37:40.8 | 57599.109500 | r | 21.14 ± 0.02 | 300 | NTT |
| 2016 Jul 30 03:16:59.5 | 57599.136800 | r | 21.15 ± 0.02 | 300 | NTT |
| 2016 Jul 30 03:21:36.0 | 57599.140000 | r | 21.09 ± 0.02 | 300 | NTT |

**Note.** PS1 and DECam photometry measured with TRIPPy (Fraser et al. 2016); NTT photometry measured with circular aperture photometry.

## ORCID iDs

Matthew J. Holman https://orcid.org/0000-0002-1139-4880
Matthew J. Payne https://orcid.org/0000-0001-5133-6303
Wesley Fraser https://orcid.org/0000-0001-6680-6558
Pedro Lacerda https://orcid.org/0000-0002-1708-4656
Michele T. Bannister https://orcid.org/0000-0003-3257-4490
Ying-Tung Chen (陳英同) https://orcid.org/0000-0001-7244-6069
Hsing Wen Lin (林省文) https://orcid.org/0000-0001-7737-6784
Rosita Kokotanekova https://orcid.org/0000-0003-4617-8878
David Young https://orcid.org/0000-0002-1229-2499
K. Chambers https://orcid.org/0000-0001-6965-7789
A. Fitzsimmons https://orcid.org/0000-0003-0250-9911
H. Flewelling https://orcid.org/0000-0002-1050-4056
Tommy Grav https://orcid.org/0000-0002-3379-0534
M. Huber https://orcid.org/0000-0003-1059-9603
Alex Krolewski https://orcid.org/0000-0003-2183-7021
R. Jedicke https://orcid.org/0000-0001-7830-028X
N. Kaiser https://orcid.org/0000-0001-6511-4306
E. Magnier https://orcid.org/0000-0002-7965-2815
M. Micheli https://orcid.org/0000-0001-7895-8209
Alex Parker https://orcid.org/0000-0002-6722-0994
Darin Ragozzine https://orcid.org/0000-0003-1080-9770
Peter Veres https://orcid.org/0000-0002-2149-9846
R. Wainscoat https://orcid.org/0000-0002-1341-0952
C. Waters https://orcid.org/0000-0003-1989-4879
R. Weryk https://orcid.org/0000-0002-0439-9341

## References

Abazajian, K. N., Adelman-McCarthy, J. K., Agüeros, M. A., et al. 2009, ApJS, 182, 543
Abolfathi, B., Aguado, D. S., Aguilar, G., et al. 2017, arXiv:1707.09322
Bannister, M. T., Alexandersen, M., Benecchi, S. D., et al. 2016a, AJ, 152, 212
Bannister, M. T., Kavelaars, J. J., Petit, J.-M., et al. 2016b, AJ, 152, 70
Bernstein, G., & Khushalani, B. 2000, AJ, 120, 3323
Brasser, R., & Morbidelli, A. 2013, Icar, 225, 40
Brown, M. E. 2008, in The Solar System Beyond Neptune, ed. M. A. Barucci et al. (Tucson, AZ: Univ. Arizona Press), 335
Brown, M. E., Bannister, M. T., Schmidt, B. P., et al. 2015, AJ, 149, 69
Brown, M. E., Burgasser, A. J., & Fraser, W. C. 2011, ApJL, 738, L26
Brown, M. E., Trujillo, C., & Rabinowitz, D. 2004, ApJ, 617, 645
Brucker, M. J., Grundy, W. M., Stansberry, J. A., et al. 2009, Icar, 201, 284
Buzzoni, B., Delabre, B., Dekker, H., et al. 1984, Msngr, 38, 9
Chambers, K. C., Magnier, E. A., Metcalfe, N., et al. 2016, arXiv:1612.05560
Chen, Y.-T., Lin, H. W., Holman, M. J., et al. 2016, ApJL, 827, L24
Denneau, L., Jedicke, R., Grav, T., et al. 2013, PASP, 125, 357
DePoy, D. L., Abbott, T., Annis, J., et al. 2008, Proc. SPIE, 7014, 70140E
Elliot, J. L., Kern, S. D., Clancy, K. B., et al. 2005, AJ, 129, 1117
Fraser, W., Alexandersen, M., Schwamb, M. E., et al. 2016, AJ, 151, 158
Fraser, W. C., Brown, M. E., & Glass, F. 2015, ApJ, 804, 1
Fraser, W. C., Brown, M. E., Morbidelli, A., Parker, A., & Batygin, K. 2014, ApJ, 782, 100
Gerdes, D. W., Sako, M., Hamilton, S., et al. 2017, ApJL, 839, L15
Gladman, B., Holman, M., Grav, T., et al. 2002, Icar, 157, 269
Gladman, B., Lawler, S. M., Petit, J.-M., et al. 2012, AJ, 144, 23
Gladman, B., Marsden, B. G., & Vanlaerhoven, C. 2008, in The Solar System Beyond Neptune, ed. M. A. Barucci et al. (Tucson, AZ: Univ. Arizona Press), 43
Gomes, R. S. 2003, Icar, 161, 404
Gomes, R. S., Fern Ndez, J. A., Gallardo, T., & Brunini, A. 2008, in The Solar System Beyond Neptune, ed. M. A. Barucci et al. (Tucson, AZ: Univ. Arizona Press), 259
Gwyn, S. D. J., Hill, N., & Kavelaars, J. J. 2012, PASP, 124, 579
Holman, M. J., Chen, Y.-T., Lin, H.-W., et al. 2015, AAS Meeting, 47, 211.12
Kaib, N. A., & Sheppard, S. S. 2016, AJ, 152, 133
Kaiser, N., Burgett, W., Chambers, K., et al. 2010, Proc. SPIE, 7733, 77330E
Kowal, C. T. 1989, Icar, 77, 118
Lacerda, P., Fornasier, S., Lellouch, E., et al. 2014, ApJL, 793, L2
Larsen, J. A., Gleason, A. E., Danzl, N. M., et al. 2001, AJ, 121, 562
Larsen, J. A., Roe, E. S., Albert, C. E., et al. 2007, AJ, 133, 1247
Lellouch, E., Santos-Sanz, P., Lacerda, P., et al. 2013, A&A, 557, A60
Lin, H. W., Chen, Y.-T., Holman, M. J., et al. 2016, AJ, 152, 147
Lineweaver, C. H., & Norman, M. 2010, arXiv:1004.1091
LSST Science Collaboration, Abell, P. A., Allison, J., et al. 2009, arXiv:0912.0201
Lykawka, P. S., & Mukai, T. 2007a, Icar, 186, 331
Lykawka, P. S., & Mukai, T. 2007b, Icar, 192, 238
Magnier, E. 2006, in The Advanced Maui Optical and Space Surveillance Technologies Conf. (Maui, HI: MEDB), 50
Magnier, E. 2007, in ASP Conf. Ser. 364, The Future of Photometric, Spectrophotometric and Polarimetric Standardization, ed. C. Sterken (San Francisco, CA: ASP), 153
Magnier, E. A., Schlafly, E., Finkbeiner, D., et al. 2013, ApJS, 205, 20
Magnier, E. A., Schlafly, E. F., Finkbeiner, D. P., et al. 2016, arXiv:1612.05242
Malhotra, R. 1995, AJ, 110, 420
Moody, R. 2004, PhD thesis, RSAA, the Australian National Univ.
Nesvorný, D., & Vokrouhlický, D. 2016, ApJ, 825, 94
Nesvorný, D., Vokrouhlický, D., & Roig, F. 2016, ApJL, 827, L35
Ofek, E. O. 2012, ApJ, 749, 10
Peixinho, N., Delsanti, A., & Doressoundiram, A. 2015, A&A, 577, A35
Petit, J.-M., Kavelaars, J. J., Gladman, B., & Loredo, T. 2008, in The Solar System Beyond Neptune, ed. M. A. Barucci et al. (Tucson, AZ: Univ. Arizona Press), 71
Petit, J.-M., Kavelaars, J. J., Gladman, B. J., et al. 2011, AJ, 142, 131
Petit, J.-M., Kavelaars, J. J., Gladman, B. J., et al. 2017, AJ, 153, 236
Pike, R. E., Fraser, W. C., Schwamb, M. E., et al. 2017a, AJ, 154, 101
Pike, R. E., Kavelaars, J. J., Petit, J.-M., et al. 2015, AJ, 149, 202
Pike, R. E., Lawler, S., Brasser, R., et al. 2017b, AJ, 153, 127

Pike, R. E., & Lawler, S. M. 2017, AJ, 154, 171
Press, W. H., & Rybicki, G. B. 1989, ApJ, 338, 277
Rabinowitz, D., Schwamb, M. E., Hadjiyska, E., & Tourtellotte, S. 2012, AJ, 144, 140
Rabinowitz, D. L., Schaefer, B. E., & Tourtellotte, S. W. 2007, AJ, 133, 26
Rein, H., & Liu, S.-F. 2012, A&A, 537, A128
Rein, H., & Spiegel, D. S. 2015, MNRAS, 446, 1424
Schaller, E. L., & Brown, M. E. 2007a, ApJL, 670, L49
Schaller, E. L., & Brown, M. E. 2007b, ApJL, 659, L61
Schwamb, M. E., Brown, M. E., & Fraser, W. C. 2013, AJ, 147, 2
Schwamb, M. E., Brown, M. E., Rabinowitz, D. L., & Ragozzine, D. 2010, ApJ, 720, 1691
Sheppard, S. S., Jewitt, D. C., Trujillo, C. A., Brown, M. J. I., & Ashley, M. C. B. 2000, AJ, 120, 2687
Sheppard, S. S., & Trujillo, C. 2016, AJ, 152, 221
Sheppard, S. S., Trujillo, C., & Tholen, D. J. 2016, ApJL, 825, L13
Sheppard, S. S., Udalski, A., Trujillo, C., et al. 2011, AJ, 142, 98
Snodgrass, C., Saviane, I., Monaco, L., & Sinclaire, P. 2008, Msngr, 132, 18
Tancredi, G., & Favre, S. 2008, Icar, 195, 851
Tegler, S. C., Grundy, W. M., Romanishin, W., et al. 2007, AJ, 133, 526
Tombaugh, C. W. 1961, in Planets and Satellites, ed. G. P. Kuiper & B. M. Middlehurst (Chicago, IL: Univ. Chicago Press), 12
Tonry, J. L., Stubbs, C. W., Lykke, K. R., et al. 2012, ApJ, 750, 99
Trujillo, C. A., & Brown, M. E. 2003, EM&P, 92, 99
Trujillo, C. A., & Sheppard, S. S. 2014, Natur, 507, 471
Volk, K., & Malhotra, R. 2017, AJ, 154, 62
Volk, K., Murray-Clay, R., Gladman, B., et al. 2016, AJ, 152, 1
Weryk, R. J., Lilly, E., Chastel, S., et al. 2016, arXiv:1607.04895